

We are IntechOpen, the world's leading publisher of Open Access books Built by scientists, for scientists

6,900

Open access books available

186,000

International authors and editors

200M

Downloads

Our authors are among the

154

Countries delivered to

TOP 1%

most cited scientists

12.2%

Contributors from top 500 universities



WEB OF SCIENCE™

Selection of our books indexed in the Book Citation Index
in Web of Science™ Core Collection (BKCI)

Interested in publishing with us?
Contact book.department@intechopen.com

Numbers displayed above are based on latest data collected.
For more information visit www.intechopen.com



Lubrication in Chemical and Mechanical Planarization

Changhong Wu and Xiaoyan Liao

Additional information is available at the end of the chapter

<http://dx.doi.org/10.5772/64484>

Abstract

Chemical mechanical planarization (CMP) has been widely used in integrated circuit (IC) processing to achieve both local and global surface planarity through combined chemical and mechanical actions. The lubrication plays a significant role in CMP and can be determined by the Stribeck curve since it provides direct evidence of the extent of contact among wafer, pad asperities, and slurry particles. The advancements in the construction of the Stribeck curve are highlighted in this chapter. Traditionally, the procedure for constructing the Stribeck curve is as follows: (1) polish wafers at various pressures and sliding velocities to obtain the coefficient of friction (COF) values; (2) plot the experimental data as COF vs. Sommerfeld number; (3) construct the Stribeck curve via curve fitting. Recently, an alternative method was presented to construct the Stribeck curve via only performing one wafer polishing experiment. Pressure and sliding velocity are varied separately or together for a desired length of time, so that multiple measurements can be taken within one run. In this study, a back-propagation (BP) neural network is proposed to construct the Stribeck curve. Results show that the BP neural network could construct a more accurate Stribeck curve and thus could better provide insight into the lubrication mechanism of CMP processes.

Keywords: chemical mechanical planarization, lubrication, Stribeck curve, neural network

1. Introduction

Integrated circuit (IC) technology plays a critical role in today's advanced industries. Since transistors were invented in the 1940s [1], IC technology has been growing nonstop. The circuit density and complexity keep on increasing driven by Moore's Law [2]. To date, the transistor count in a central processing unit (CPU) can reach up to several billions [3]; the commercial technology node scales down to 14 nm and the maximum wiring layer is 13 [4]. High volume

manufacturing of ICs relies heavily on the advancements in each unit process such as chemical mechanical planarization (CMP), lithography, etching, deposition, and cleaning. Among these processes, CMP has been an enabling technology in the realization of IC manufacturing. Presently, CMP is the only planarization technique that can offer excellent local and global planarity. For the most advanced ultra-large-scale integration (ULSI), CMP is the only choice for global surface planarization [5]. In this chapter, the lubrication of CMP is reviewed. Particularly, the advancements in the construction of Stribeck curve are highlighted.

2. What is CMP?

CMP typically refers to chemical mechanical planarization. As its name indicates, CMP simultaneously employs both chemical and mechanical actions to selectively remove the exposed material from elevated features for improved planarization [6–14]. Driven with the planarization challenge in IC manufacturing for smaller minimum feature size and more wiring levels, CMP was invented by International Business Machines (IBM) in the mid-1980s [15].

Figure 1 schematically shows a generalized CMP process on a rotary polisher. The wafer to be polished is secured by a retaining ring, which is attached to the carrier head. The rotating wafer is pressed against the rotating polishing pad under a certain pressure from the carrier head [5, 7]. Slurry, containing chemicals and nanoparticles, is injected onto the pad surface and transported to the pad-wafer interface through platen-wafer rotation, pad surface structures as well as the retaining ring. Slurry chemicals react with the wafer surface to form a softer porous layer, which is then removed by mechanical forces generated among wafer surface, pad asperities, and slurry nanoparticles. In addition, a pad conditioner is typically used to refresh pad asperities and keep material removal rate stable [5, 7, 13, 14].

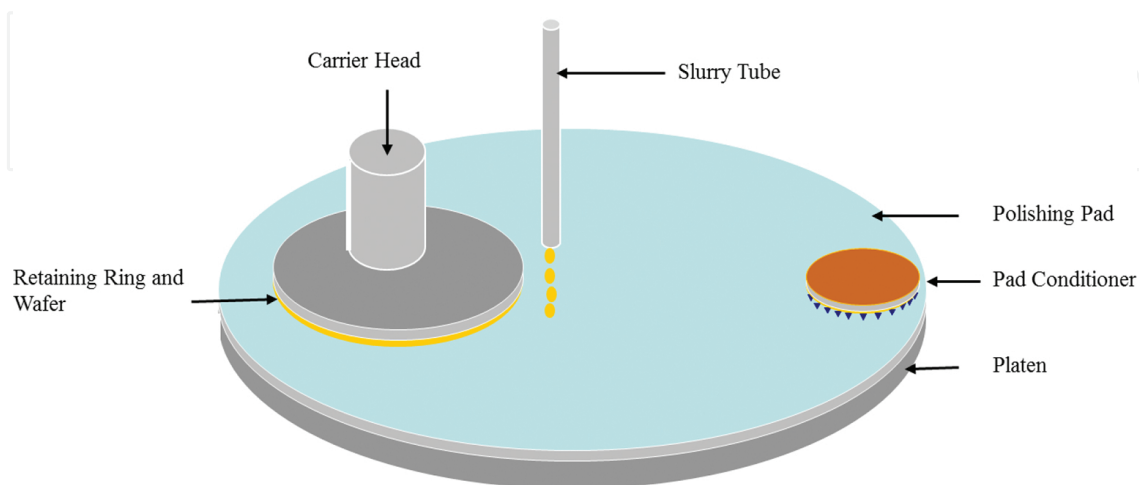


Figure 1. Schematic of a generalized CMP process on a rotary polisher [7].

3. Stribeck curve

Tribology is generally understood as the science and technology of interacting surfaces in relative motion [16]. As schematically shown in **Figure 2**, three-body (i.e., wafer, pad, and slurry particles) contact occurs in CMP. Tribology, including friction, lubrication, and wear, plays a crucial role in CMP [16]. In this chapter, we will focus on the lubrication in CMP.

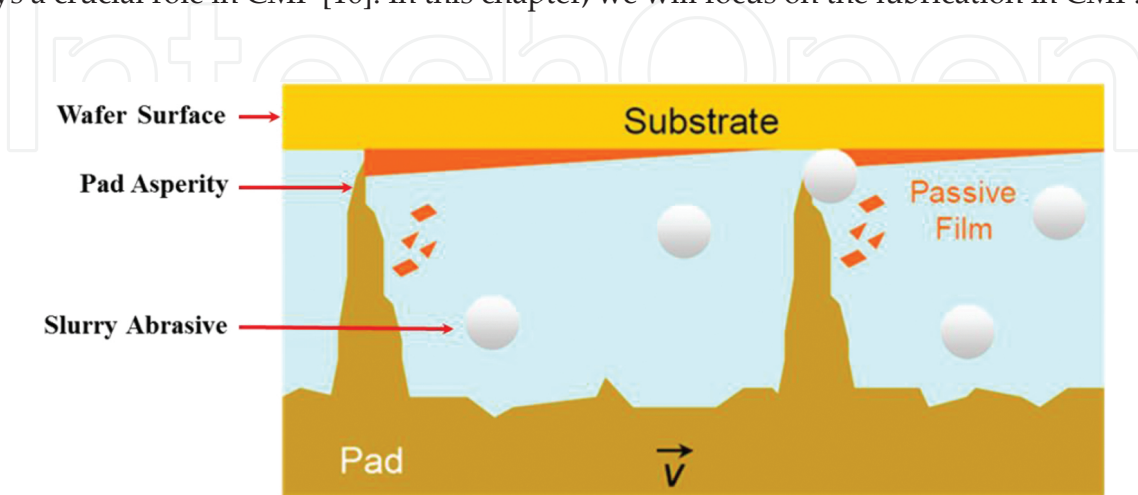


Figure 2. Schematic of three-body contact in CMP [17].

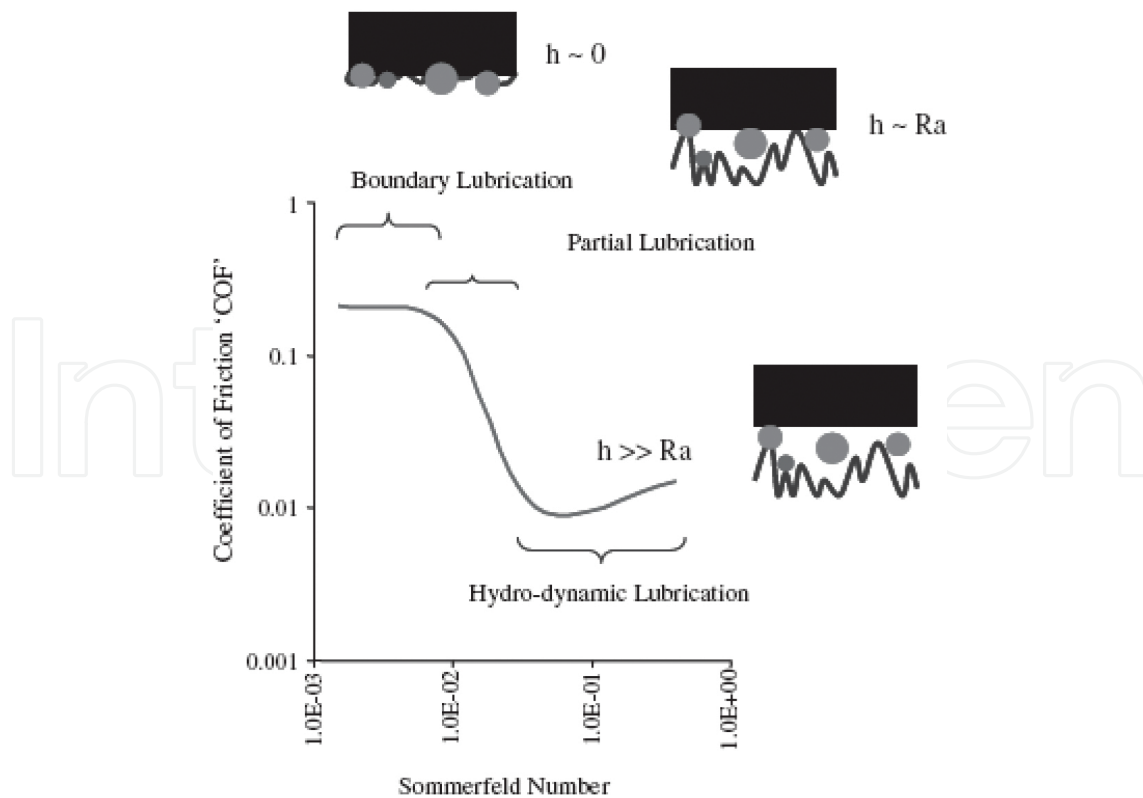


Figure 3. Generic Stribeck curve based on Sommerfeld number [18].

The lubrication mechanism in CMP processes can be determined by the Stribeck curve [18]. **Figure 3** shows a generic Stribeck curve based on Sommerfeld number [18]. In this figure, Y axis is coefficient of friction (COF), and X axis represents the Sommerfeld number. COF is defined as the ratio of the shear force to the down force. During CMP, shear force is generated among the wafer, pad asperities, and slurry nanoparticles. The shear force and down force can be measured using appropriate instruments such as CETR CP4 and Araca APD-800 [5, 19]. For example, using Araca APD-800, **Figure 4** shows the transient shear force and down force as a function of polishing time, and **Figure 5** shows the transient COF. Since COF is defined as the ratio of the shear force to the down force, the transient COF can be expressed as:

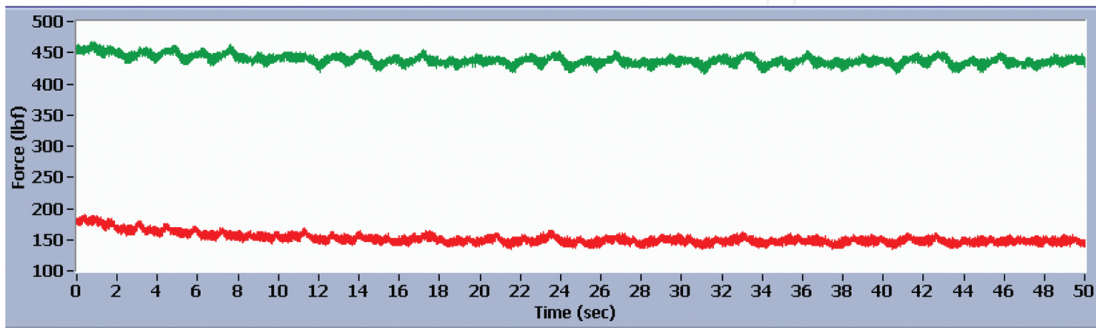


Figure 4. The transient shear force and down force as a function of polishing time [5].

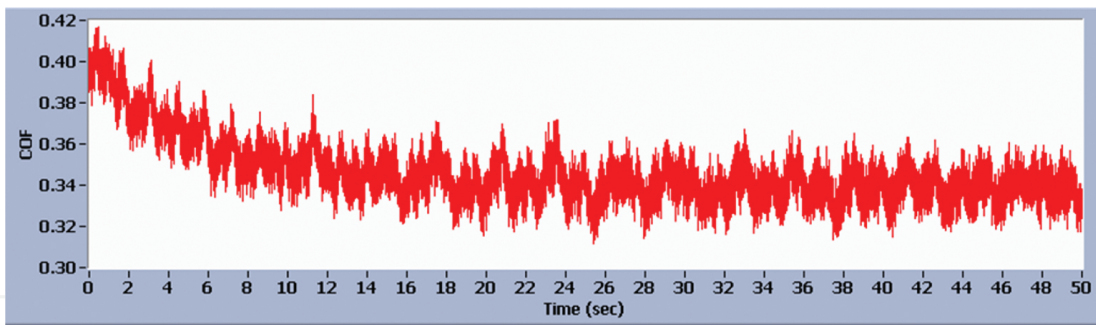


Figure 5. Transient COF based on **Figure 4** [5].

$$COF_i = \frac{\text{Shear force}_i}{\text{Down force}_i} \quad (1)$$

In **Figure 3**, X axis is the Sommerfeld number (S_o), which is defined as follows [18]:

$$S_o = \frac{\mu V}{p \delta_{eff}} \quad (2)$$

where μ is the viscosity of slurry, V is the pad-wafer sliding velocity, p is the wafer pressure, and δ_{eff} is the effective slurry film thickness at the wafer and pad interface.

Slurry viscosity μ can be measured experimentally, and the pad-wafer sliding velocity V can be calculated based on the tool geometry and the relative angular velocity of the wafer and platen [18]. The wafer pressure p is the applied down force divided by the contact area between the wafer and pad. Finally, the effective slurry film thickness δ_{eff} can be assumed as the arithmetic average roughness of the pad based on slurry film thickness measurement results by dual emission laser induced fluorescence (DELIF) [20–22]. In some cases, the pseudo Sommerfeld number (V/p) is used to replace Sommerfeld number for simplicity [23].

As mentioned previously, the lubrication mechanism in CMP processes can be determined by the Stribeck curve since it provides direct evidence of the extent of contact among wafer, pad asperities, and slurry particles [18]. As evident from **Figure 3**, there are three contact modes: boundary lubrication, partial lubrication, and hydro-dynamic lubrication.

Boundary lubrication occurs at smaller values of the Sommerfeld number. In this regime, the slurry film is quite thin, and thus, the wafer, pad, and slurry particles are intimate contact with one another [18]. COF is high and independent of the Sommerfeld number. From a process control point of view, the boundary lubrication is preferable because of its high and stable COF [7].

The partial lubrication occurs at intermediate values of the Sommerfeld number. In this regime, the slurry film thickness is similar to that of the roughness of the pad [18]. The slurry film layer partially separates the wafer and pad, and COF sharply drops as increase in the Sommerfeld number. A small change in process parameter such as polish pressure and velocity may cause a significant change in COF.

Hydro-dynamic lubrication occurs at larger values of the Sommerfeld number. In this regime, the slurry film thickness is larger than that of the roughness of the pad [18]. As such, very little contact exists between the wafer and pad. COF is small and increases slightly as increase in the Sommerfeld number [5].

Since the Stribeck curve can determine the lubrication mechanism in CMP processes, it has many practical applications. For example, it can help screen certain consumable sets (pad, slurry, wafer, retaining ring, etc.) by determining whether and how they contact one another during CMP. It can also help determine the optimal polish parameters (wafer and retaining ring pressure, pad/wafer velocity, slurry flow rate, etc.) [24].

4. Advancements in Stribeck curve construction

Traditionally, the procedure of constructing the Stribeck curve for a given consumables set is as follows [25]: (1) polishing wafers at various pressures and sliding velocities. One or more wafers typically need to be polished to obtain the COF at each given polish pressure and sliding velocity; (2) plotting experimental data as COF vs. Sommerfeld number or pseudo Sommerfeld

number (V/p); and (3) performing curve fitting or simply connecting data points to obtain the Stribeck curve.

Figure 6 shows Stribeck curves where oxide wafers were polished on different types of pads using Fujimi PL-4217 slurry with 25% abrasives. As evident from **Figure 6**, the relationship between COF and Sommerfeld number is complicated. First, for a given consumables set, this relationship needs to be described using different mathematical functions depending on the lubrication regions. Second, as shown in **Figure 6**, this relationship varies with consumables set (pad in this case). A process could fall in different lubrication regions for different consumable sets at the same Sommerfeld number. For example, when Sommerfeld number ranges from 0.0002 to 0.0008, IC 1400 k-groove pad and IC 1000 perforated pad are in the boundary and partial lubrication region, respectively. As such, it is difficult to describe the relationship between COF and Sommerfeld number using a general explicit function. This renders challenges to curve fitting for the Stribeck curve construction, which needs to predetermine the form of function. On the other hand, if we just simply connect data points to obtain the Stribeck curve, it could be not accurate if the data points are not enough.

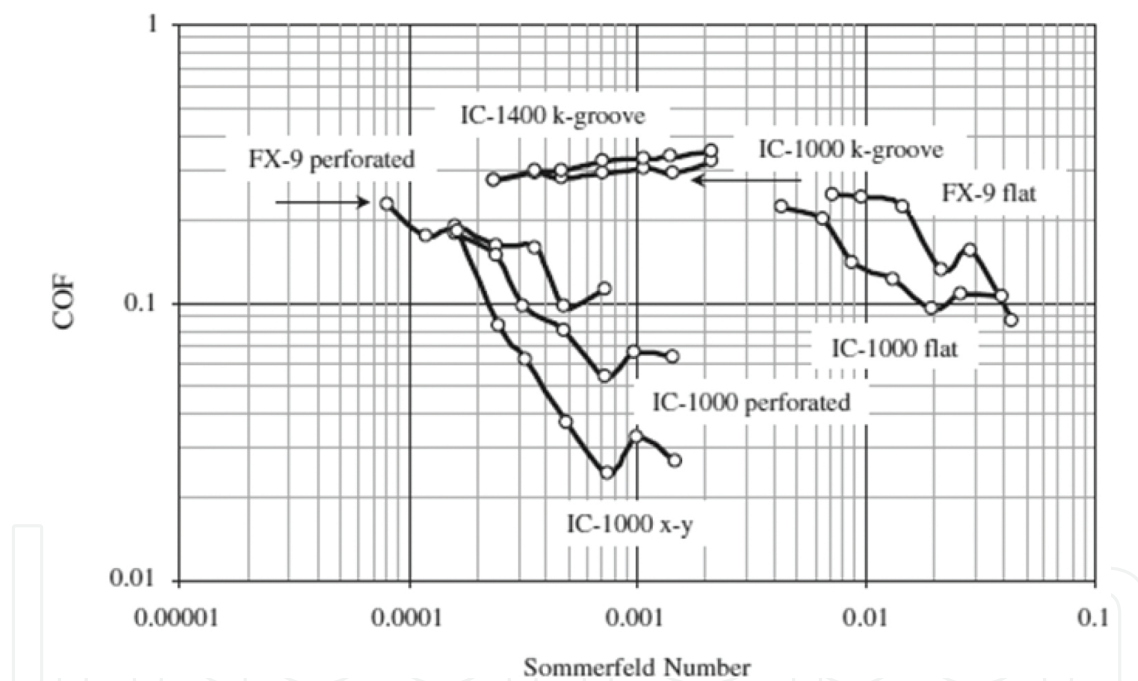
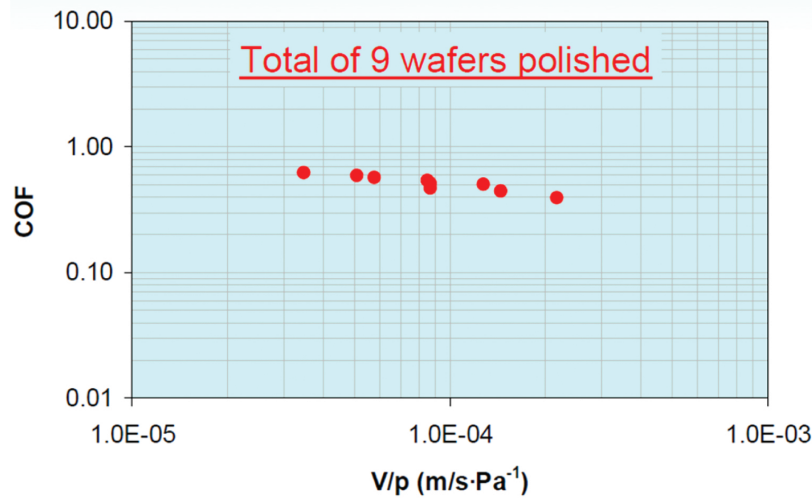


Figure 6. Stribeck curves at 25% abrasives with Fujimi PL-4217 slurry [18].

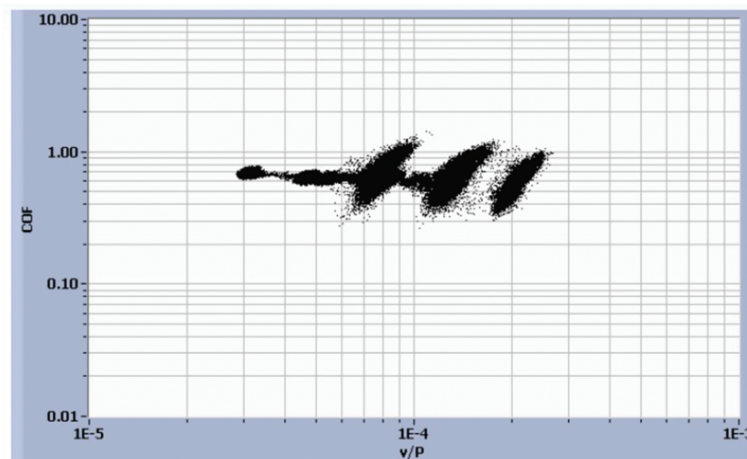
Zhuang and Jiao et al. proposed an alternative method to construct the Stribeck curve by only performing one wafer polishing experiment [23, 24]. Pressure and sliding velocity are varied separately or together for a desired length of time, so that multiple measurements (COF , V , p) can be taken within one run. This is attributed to their polisher (i.e., Araca APD-800), which is capable of measuring shear force, down force, and rendering a value for COF in real time.

Figure 7(a) shows the 'traditional' Stribeck curve. Three hundred-millimeter blanket copper wafers were polished on a Cabot Microelectronics Corporation (CMC) D100 pad with CMC

EP-C600Y-75 slurry at different polish pressures (1.0–2.5 psi) and sliding velocities (0.6–1.5 m/s). One wafer was polished for each particular V and p combination, and totally, nine wafers were polished. In comparison, **Figure 7(b)** shows the Stribeck curve obtained by the new method where only one wafer was polished in the range of V/p investigated. As observed in **Figure 7**, the CMP process is in the boundary lubrication. Also, it should be noted that the new method can collect enough data by only polishing one wafer and thus does not need to perform curve fitting to obtain the Stribeck curve.



(a)



(b)

Figure 7. Stribeck curves obtained by the (a) traditional and (b) new method on D100 pad [24].

Figure 8(a) and **(b)** shows another example of Stribeck curves, which were obtained by the traditional and new method, respectively. Polishing conditions and consumables in **Figure 8** were same as **Figure 7** except that Dow IC 1000 k-groove pad was employed in **Figure 8**. As observed in **Figure 8**, the CMP process is in the partial lubrication. As we can see, the change in the type of the pad, the lubrication mechanisms of the CMP processes may change.

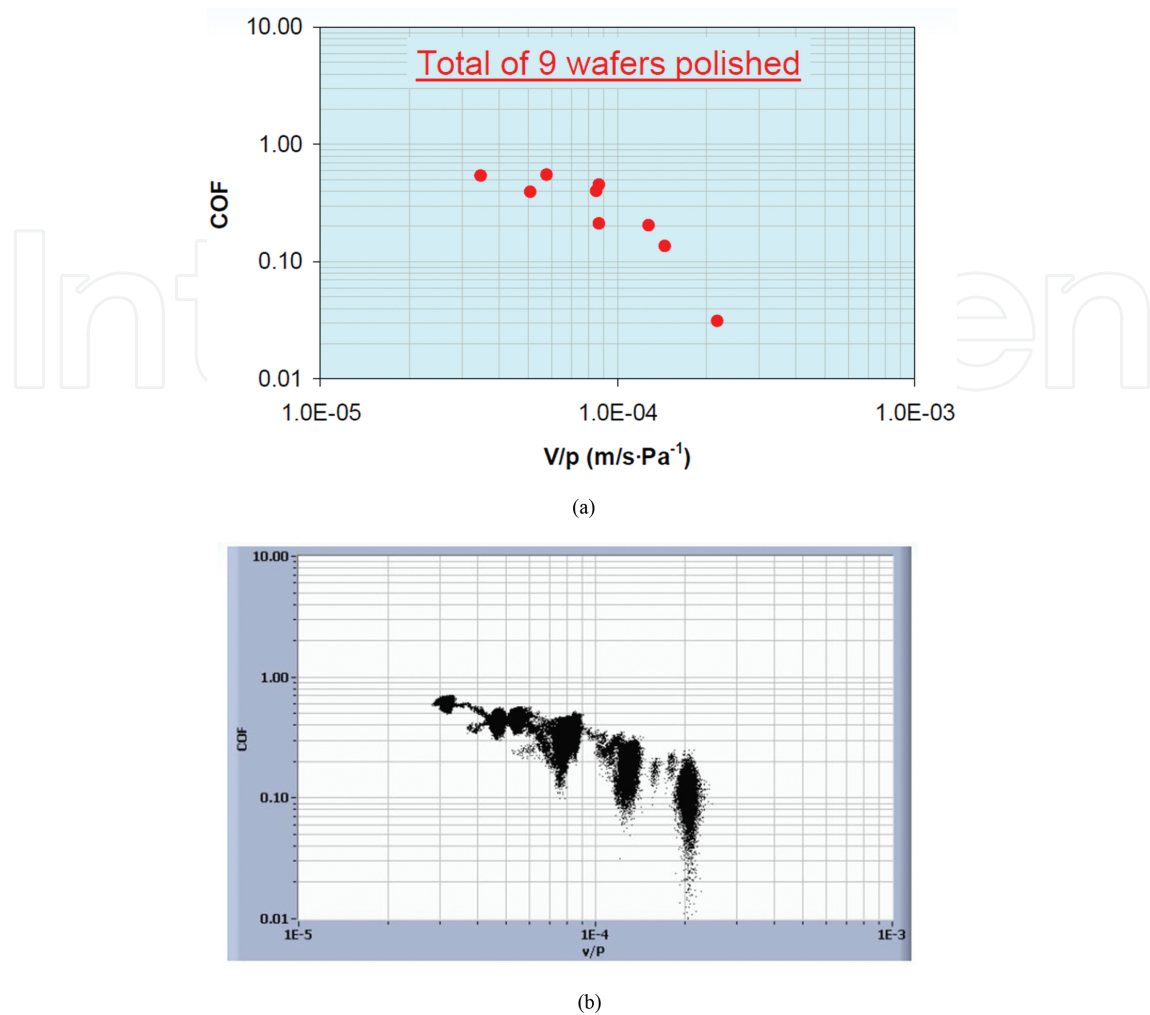


Figure 8. Stribeck curves obtained by the (a) traditional and (b) new method on IC 1000 pad [24].

5. Artificial neural network for Stribeck curve

The above new method proposed by Zhuang and Jiao *et al.* can provide an accurate Stribeck curve. As mentioned previously, this is attributed to their polisher which is capable of measuring shear force, down force, and rendering a value for COF in real time. Due to the limitation of the experimental apparatus, the traditional method (i.e., polishing one wafer at each given pressure and velocity) is still commonly used. To construct an accurate Stribeck curve based on the limited data points (COF vs. V/p), which are obtained by the traditional method, a new neural network-based method is presented here.

Artificial neural networks have been widely used for nonlinear function approximation, pattern identification, system modeling, and control [25–33]. For example, Wu *et al.* employed the neural network to predict molten temperature of blended coal ash and estimate the degree of slagging of the coal-fired boiler in power plant [29, 30]. Furthermore, Wu *et al.* optimized

power coal blending based on neural network and genetic algorithm [28, 32]. These successful work provided a method for the construction of Stribeck curve in this study.

There are various types of neural networks such as back-propagation (BP), linear, and RBF neural networks. Among these networks, BP neural network is the most widely used one. In this chapter, a BP neural network is employed to construct the Stribeck curve.

Figure 9 schematically shows the architecture of a 3-layer BP neural network. The first layer (i.e., input layer) and the last layer (i.e., output layer) consist of the independent and dependent variables, respectively. The dependent variables in the output layer are determined by the independent variables in the input layer [26]. In Stribeck curve, COF is shown as a function of Sommerfeld number or pseudo Sommerfeld number (V/p). Therefore, the input layer of the neural network is V/p and the output layer is COF.

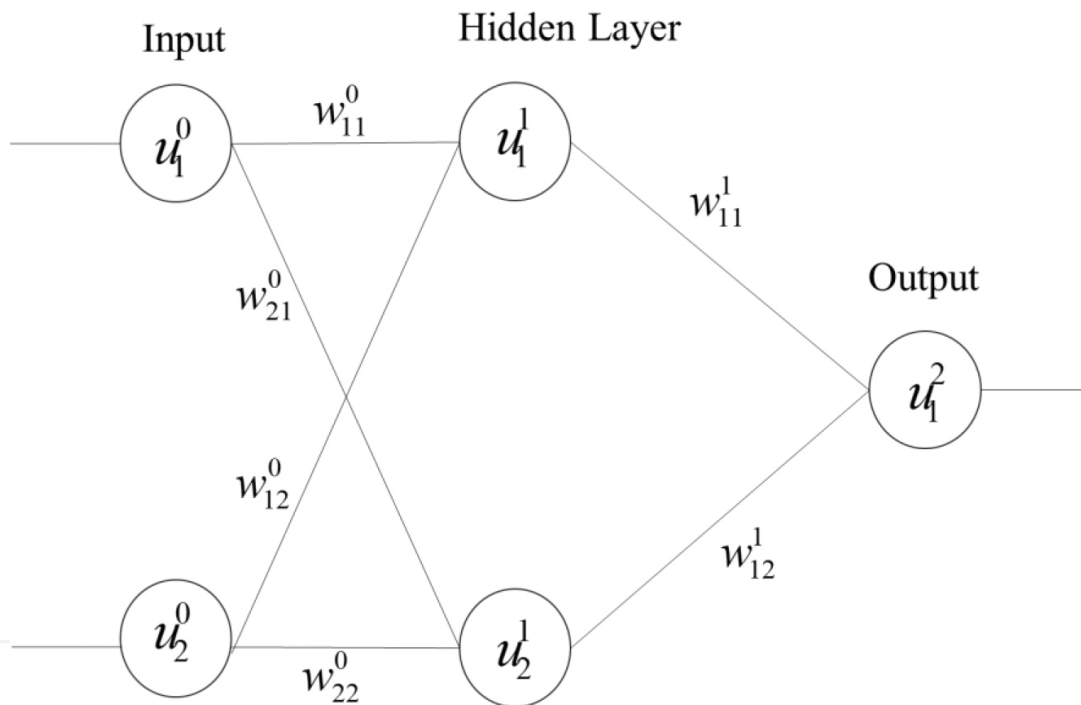


Figure 9. Architecture of a three-layer BP neural network.

For BP neural network, transfer functions ('tansig,' 'purelin,' 'logsig,' etc.) are used to transfer data from one layer to the next layer. The BP algorithm for neural network training was described in detail in Ref. [34]. The main procedure is [28–34]: at first, the weights (w_{ik}) and biases of the network are initialized. A certain amount of samples is then used for training. The values of the input and output of the training samples are already known. Outputs of the training samples are calculated based on the inputs, weights, and biases. Then, the network outputs and the real outputs of the training samples are compared to calculate the error. If the error meets the target, the training is completed. If not, the weights and biases of the network need to be adjusted and the outputs and errors are recalculated. Repeat the above procedure

until the error goal is met. After training, it is expected that the neural network can predict the value of the output when a new value of the input is given.

A case study is presented here. Three-layer BP neural network is employed to construct the Stribeck curve. Both input layer and output layer have only one neuron, and the number of neuron in the hidden layer is selected as 4. The nine data points in **Figure 7(a)** are used as the training samples. For the input, $V/p = [0.000035 \ 0.000051 \ 0.000058 \ 0.000084 \ 0.000086 \ 0.000087 \ 0.00012 \ 0.00014 \ 0.00021]$; for the output, $\text{COF} = [0.64 \ 0.6 \ 0.57 \ 0.54 \ 0.51 \ 0.47 \ 0.5 \ 0.44 \ 0.4]$. The error goal is set as 10^{-5} , the transform function from the input layer to hidden layer is 'tansig,' and the one from the hidden layer to output layer is 'purelin.'

After training, the neural network is used to predict COF for a particular combination of pressure and velocity. In this case, the COF values are predicted with a V/p interval of 10^{-5} from 0.000035 to 0.00021. The prediction COF values obtained by the neural network are plotted as a function of V/p , as shown in **Figure 10** (see the blue curve). As we can see, the prediction COF values agree well with the actual COF values (see the circles) of the training samples. If we compare the Stribeck curve obtained by the neural network in **Figure 10** with the Stribeck curve obtained by the experimental approach in **Figure 7(b)**, they are consistent. Therefore, after training, the neural network can successfully capture the nonlinear relationship between the input and output. COF for a particular combination of pressure and velocity can be accurately predicted by the neural network. We believe that the successful construction of the Stribeck curve by the BP neural network could better provide insight into the lubrication mechanism of CMP processes.

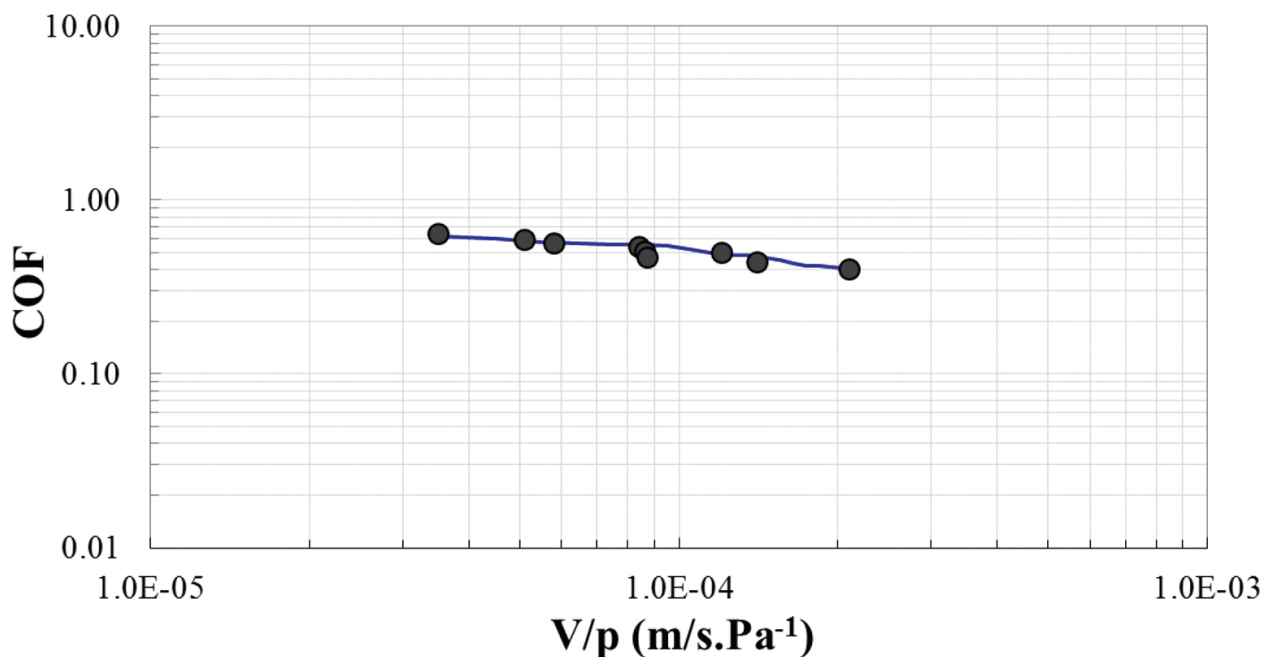


Figure 10. Stribeck curves obtained by the neural network.

Author details

Changhong Wu¹ and Xiaoyan Liao^{2*}

*Address all correspondence to: xiaoyan@email.arizona.edu

1 Advanced Technology Development (ATD), GLOBALFOUNDRIES, Malta, NY, USA

2 School of Chemical Engineering and Energy, Zhengzhou University, Zhengzhou, Henan, China

References

- [1] W. Shockley, "The path to the conception of the junction transistor", *IEEE Trans. Elec. Dev.*, ED-31, 1523 (1984).
- [2] G. Moore, "Cramming more components onto integrated circuits", *Electronics*, 38 p. 114-117 (1965).
- [3] V. Krishnaswamy, L. Shin, and S. Turullols, 9th IEEE Asian Solid-State Circuits Conference Proceedings of Technical Papers, Sentosa Island, Singapore; p. 17 (2013).
- [4] <http://www.itrs.net/>
- [5] C. Wu, "Control of slurry flow, temperature and aggressive diamonds in chemical mechanical planarization", Ph.D. Thesis, University of Arizona, Tucson, AZ (2015).
- [6] J. Steigerwald, S. Murarka, and R. Gutmann, *Chemical Mechanical Planarization of Microelectronic Materials*, Wiley, NY (1997).
- [7] X. Liao, "Process optimization and fundamental consumables characterization of advanced dielectric and metal chemical mechanical planarization", Ph.D. Thesis, University of Arizona, Tucson, AZ (2014).
- [8] X. Liao, Y. Zhuang, L. Borucki, J. Cheng, S. Theng, T. Ashizawa, and A. Philipossian, "Effect of pad surface micro-texture on removal rate during interlayer dielectric chemical mechanical planarization process", *Jpn. J. Appl. Phys.*, 52, 018001 (2013).
- [9] X. Liao, Y. Zhuang, L. Borucki, J. Cheng, S. Theng, T. Ashizawa, and A. Philipossian, "Effect of pad surface micro-texture on wafer topography during shallow trench isolation chemical mechanical planarization process", *Jpn. J. Appl. Phys.*, 53, 086501 (2014).
- [10] X. Liao, Y. Zhuang, L. Borucki, S. Theng, X. Wei, T. Ashizawa, and A. Philipossian, "Effect of pad surface micro-texture on coefficient of friction and removal rate during copper CMP process", *Electrochem. Solid-State Lett.*, 14, H201 (2011).

- [11] X. Liao, Y. Sampurno, Y. Zhuang, and A. Philipossian, "Effect of slurry application/injection schemes on slurry availability during chemical mechanical planarization (CMP)", *Electrochem. Solid-State Lett.*, 15, H118 (2012).
- [12] C. Wu, Y. Sampurno, X. Liao, Y. Jiao, S. Theng, Y. Zhuang, L. Borucki, and A. Philipossian, "Pad surface thermal management during copper chemical mechanical planarization", *ECS J. Solid State Sci. Technol.*, 4(7), P206-P212 (2015).
- [13] C. Wu, Y. Sampurno, X. Liao, Y. Zhuang, L. Borucki, S. Theng, and A. Philipossian, "Effect of pad groove design on slurry injection scheme during interlayer dielectric chemical mechanical planarization", *ECS J. Solid State Sci. Technol.*, 4(7), P272-P276 (2015).
- [14] C. Wu, Y. Zhuang, X. Liao, Y. Jiao, Y. Sampurno, S. Theng, F. Sun, A. Naman, and A. Philipossian, "Aggressive diamond characterization and wear analysis during chemical mechanical planarization", *ECS J. Solid State Sci. Technol.*, 2(1), P36-P41 (2013).
- [15] D. Moy, M. Schadt, C. Hu, F. Kaufman, A. Ray, N. Mazzeo, E. Baran, and D. Pearson, Proceedings 1989 VMIC Conference, Santa Clara, CA, US; p. 26 (1989).
- [16] H. Liang and D. Craven, *Tribology in Chemical Mechanical Planarization*, Taylor & Francis, Boca Raton, FL (2005).
- [17] D. DeNardis, "Evaluation and modeling of alternative copper and inter-layer dielectric chemical mechanical planarization technologies", Ph.D. Thesis, University of Arizona, Tucson, AZ (2006).
- [18] A. Philipossian and S. Olsen, "Fundamental tribological and removal rate studies of inter-layer dielectric chemical mechanical planarization", *Jpn. J. Appl. Phys.*, 42, 6371-6379 (2003).
- [19] <http://www.cetr.com/>
- [20] A. Lawing, Proceedings of 7th International Chemical-Mechanical Planarization for ULSI Multilevel Interconnection Conference (CMP-MIC), Fremont, CA, US; p. 1 (2002).
- [21] J. Lu, J. Coppeta, C. Rogers, V. Manno, L. Racz, and A. Philipossian, The Effect of Wafer Shape on Slurry Film Thickness and Friction Coefficients in CMP *Mater. Res. Soc. Symp. Proc.*, 613, E1.2.1 (2000).
- [22] C. Rogers, J. Coppeta, and L. Racz, Analysis of Flow Between a Wafer and Pad During CMP Processes *J. Electron. Mater.*, 27, 1082 (1998).
- [23] Y. Jiao, X. Liao, C. Wu, S. Theng, Y. Zhuang, Y. Sampurno, M. Goldstein, and A. Philipossian, "Tribological, thermal and kinetic attributes of 300 vs. 450 mm chemical mechanical planarization processes", *J. Electrochem. Soc.*, 159, H255 (2012).
- [24] Y. Zhuang, ERC TeleSeminars, May 29, 2010.

- [25] J. Yi, Y. Sheng, and C. Xu, "Neural network based uniformity pro-file control of linear chemical-mechanical planarization", *IEEE Trans. Semicond. Manuf.*, 16, 609-620 (2003).
- [26] X. Liao, C. Wu, and J. Zheng, "New neural network-based method for Stribeck curve construction during chemical mechanical planarization", The International Semiconductor Technology Conference/China Semiconductor Technology International Conference (ISTC/CSTIC 2016), Shanghai, China, March 13–14 (2016).
- [27] G. Wang and C. Yu, "Developing a neural network-based run-to-run process controller for chemical-mechanical planarization", *Int. J. Adv. Manuf. Technol.*, 28, 899-908 (2006).
- [28] Y. Liao, C. Wu, and X. Ma, "New hybrid optimization model for power coal blending", Proceedings of 2005 International Conference on Machine Learning and Cybernetics, Guangzhou, August 18, vol. 7, pp. 4023-4027 (2005).
- [29] C. Wu, X. Ma, and Y. Liao, "Forecasting slagging of coal-fired boiler in power plant based on fuzzy network", *J. Combust. Sci. Technol.*, 2, 17 (2006).
- [30] C. Wu and X. Ma, "Experimental research and forecast of the softening temperature of blended coal ash", *J. Eng. Therm. Power.*, 21, 179 (2006).
- [31] C. Wu, X. Ma, Z. Dong, Z. Zhao, H. Li and Y. Chen, "Study on NO emission from co-combustion of plastic powder and rice hull in CFB", *Trans. Chin. Soc. Agr. Machin.*, 38, 92-97 (2007).
- [32] Y. Liao, C. Wu, and X. Ma, "Research on optimization model for power coal blending based on genetic algorithm", ASME 2005 Power Conference, Guangzhou, China pp. P203-P207 (2005).
- [33] X. Liao, H. Zou, and C. Wu, "Research on NO_x emissions from co-combustion of wood powder and plastic powder in CFB", *Boiler Technol.*, 37, P72-P76 (2006).
- [34] X. Wen, L. Zhou, and X. Li. MATLAB Neural Network Simulation and Application, Chinese Science Press, Beijing, China (2003).

IntechOpen

